Two-dimensional collective flux pinning, defects, and structural relaxation in amorphous superconducting films

P. H. Kes* and C. C. Tsuei
IBM Thomas J. Watson Research Center, Yorktown Heights, New York 10598
(Received 28 February 1983)

The existence of two-dimensional collective pinning has been experimentally confirmed by measuring the pinning force F_p in superconducting amorphous films of transition-metal—metalloid alloys (Nb_3Ge, Nb_3Si, Mo_3Si) as a function of perpendicular field, temperature, and thickness of the specimens. The field and temperature dependence of F_p can be well explained if it is assumed that the pinning defects in these amorphous superconductors are quasidislocation loops of sizes comparable to the superconducting coherence length. Structural relaxation studies in Nb_3Ge show that these defects are stable against annealing at temperatures up to at least 0.8 of the recrystallization temperature. The possible effect of randomly distributed pinning centers (random field) on the phase transitions of a two-dimensional flux-line lattice is briefly discussed.

I. INTRODUCTION

Recently we reported on some experimental evidence for two-dimensional (2D) collective pinning in amorphous superconductors[1] (henceforth referred to as I). The concept of collective pinning, introduced by Larkin and Ovchinnikov[2] (LO), explains flux pinning in terms of the break down of the long-range positional order of the flux-line lattice[3] (FLL) due to the interaction with a dense system of randomly distributed pinning centers. The FLL spontaneously breaks up into domains or correlated regions in which short-range order persists. The correlation lengths perpendicular to and parallel with the field directions are, respectively, denoted by R_c and L_c. The net pinning force on a domain is proportional to $N^{1/2}$, where N is the number of pinning centers per domain. In this sense the LO theory is a special case of a more general theory, the random-field model[4] that describes various systems in condensed-matter physics.[5]

Owing to its statistical character, collective pinning does not require a threshold criterion, which is typical for single-particle pinning[2] in dilute pinning systems.[6,7] As clearly demonstrated by Kramer,[8] most strong pinning systems do not fulfill this threshold criterion. The only experimental evidence for the existence of a threshold was obtained by Kerchner *et al.*[9] very close to the upper critical field in a carefully prepared Nb sample with extremely small critical currents at lower fields. In other model pinning systems (Nb with either dislocation loops or voids as the major pinning centers[8]) the 3D LO collective pinning theory predicts volume pinning forces several orders of magnitude smaller than observed experimentally. This discrepancy originates most likely from the role defects of the FLL (FLD) play in the pinning phenomena, leading to a decrease of the correlation lengths and of the effective elastic moduli of the FLL.[10] To understand flux pinning it is of great importance to confirm experimentally that collective pinning does exist in systems where FLD are not likely to occur, namely, in materials that exhibit an *a priori* small critical current. We chose therefore amorphous transition-metal-based (TM) superconductors, such as amorphous Nb_3Ge, Nb_3Si, and Mo_3Si in the form of sputtered thin films with thickness ranging from 0.2 to 3 μm. In I we briefly pointed out the advantageous properties of these materials which make them very good candidates for observing collective pinning. Some of the requirements and corresponding characteristics are dealt with in more detail in Sec. II.

Because of the geometry of the experiment in which the magnetic field is applied perpendicular to the film surface, the weak pinning, and the relatively large tilt modulus of the FLL,[11] c_{44}, no serious distortions can develop along the field direction. As a result, $L_c \gg d$, the thickness of the sample, so that the flux-pinning problem becomes two dimensional and the only relevant elastic modulus of the FLL that remains is the shear modulus c_{66}. The formulas for 2D collective pinning are relatively simple. The only parameter of the theory is the quantity $W(0) \equiv n_v \langle f^2 \rangle$, where n_v is the volume density of pinning centers with elementary interaction f. The average is taken over a lattice cell of the FLL. A derivation is given in Appendix B. The experimental results and their qualitative analysis in terms of the 2D LO theory are presented in Sec. III A. An enhancement of the observed pinning force above the 2D LO prediction on approaching the upper critical field $\mu_0 H_{c2}$ is explained by a reduction of the shear modulus due to the increasing disorder in the FLL.[1] This softening of the shear modulus is discussed in Sec. III B. The properties of the FLL very close to $\mu_0 H_{c2}$ and at very small fields are treated, respectively, in Secs. III C and III D. Straight flux lines in a thin film form a 2D lattice in which topological phase transitions are theoretically predicted.[12] In Sec. III E we investigate the possibility of explaining the peak close to $\mu_0 H_{c2}$ in terms of the theory for 2D melting.[13,14] The condition for the occurrence of 2D collective pinning ($L_c \gg d$) is expressed in Sec. III F in experimentally accessible quantities.

Section IV is devoted to a discussion of the origin of the elementary pinning interaction in the amorphous superconductors we studied in this work. It provides important information about the defect structure of transition-metal glasses which can be compared with computer simulations[15] and models developed for ferromagnetic glasses.[16] Additional information on the defect structure and the su-

perconducting properties after structural relaxation is obtained from an annealing sequence carried out on one of the Nb_3Ge samples at a temperature well below the glass temperature. The results of this and some other structural relaxation experiments are presented and discussed in Sec. V.

II. SAMPLE PREPARATION AND CHARACTERISTICS

The amorphous Nb_xGe, Nb_xSi, and Mo_xSi (nominally denoted by $x=3$) samples were prepared by rf sputtering in krypton on sapphire substrates cooled by liquid nitrogen[17] (typical rate ~ 4 Å/s). The composition of these alloys as determined by electron microprobe analysis was, respectively, $x=3.6$, 2.8, and 3.5. No detectable amounts of krypton or oxygen could be traced within the resolution of, respectively, 0.1 and 0.5 wt. %. Metal masks provided strips of 4×22 mm. The amorphousness of the thicker samples was checked by large-angle x-ray scattering experiments.[17] We also prepared some thin (up to 30 nm) Nb_3Ge layers on silicide windows (thickness of 50 nm) for transmission electron microscopy (TEM). No traces of any microcrystalline structure could be detected within the experimental resolution of 1 nm and 1 vol. %.

The samples were mounted on a copper block with a backing of thermal compound in between. The temperature in ambient field was determined with a calibrated Ge sensor. In applied fields it was controlled by means of an electronic feedback system consisting of a capacitor sensor, a Lake Shore controller, and a heater on the copper block. The sample surface was perpendicular to the axis of a 9-T superconducting magnet. The resistivity and the critical current measurements were carried out in a four-point geometry with a spacing of 6 mm between the voltage probes (spring contacts). In some cases (Nb_3Si 27C and 31B) indium pressure contacts were used. The thickness was measured with a Tencor alpha-step thickness monitor.

It is experimentally established that these materials are weak-coupling type-II superconductors in the extreme dirty limit.[18] This feature enables us to determine several important superconductor parameters from theoretical expressions, such as the Ginsburg-Landau (GL) parameter κ, the coherence length $\xi(0)$, the penetration depth $\lambda(0)$, and the thermodynamic critical field $\mu_0 H_c(0)$ at $T=0$. A summary of these expressions and their sources is given in Appendix A. It shows that the only experimental quantities required are the critical temperature T_c, the resistivity ρ_0, and the slope of the upper critical field $\mu_0 H_{c2}$ vs T at T_c: $-\mu_0 dH_{c2}/dT\,|_{T_c}$. A survey of the properties of all the as-received samples on which we report here is given in Table I. The computed density of states (not listed in Table I) for amorphous Nb_3Ge, $N^*(0)=2.22\times 10^{47}$ states $J^{-1}\,m^{-3}\,spin^{-1}$, is consistent with the measured Sommerfeld constant for this material.[19]

The transition temperature was defined as the midpoint of the measured $R(T)$ curve and the transition width ΔT_c as the temperature difference between $0.1R_n$ and $0.9R_n$, where R_n is the normal-state resistance. Apparently, from ΔT_c, the thicker samples are somewhat less uniform, probably due to fluctuations in the chemical order supposedly related to the less constant sputtering conditions during longer deposition times (for instance, 100 min for Nb_3Ge 176A). The superconductor characteristics of Nb_3Ge and Nb_3Si are almost equivalent, Mo_3Si, however, has a T_c and $B_c(0)$ roughly twice as large.

The requirements to observe 2D collective pinning are, in addition to the condition $L_c \gg d$: (i) no single-particle pinning, (ii) no FLD, (iii) no edge pinning, and (iv) no pinning by surface roughness. The condition $L_c \gg d$ can only be checked retrospectively, but turns out to hold for all our samples as will be shown in Sec. III F. It is very likely from the relatively low critical currents J_c encountered in these materials,[20] that single-particle pinning and FLD are not significant. Owing to the experimental geometry the applied magnetic field $\mu_0 H_a$ must be equal to the flux density B in the sample. Under the condition $2\pi\lambda \gg a_0 = 1.07(\Phi_0/B)^{1/2}$ (a_0 is the FLL parameter and Φ_0 the flux quantum), it is found from the work of Brandt[21] (see also p. 341 of Ref. 7) that the contribution due to edge pinning is negligibly small. Because in our samples λ and $-\mu_0 dH_{c2}/dT\,|_{T_c}$ are so large, the condition $2\pi\lambda \gg a_0$ is not fulfilled only close to T_c for small reduced fields $b=B/B_{c2} \lesssim 0.1$ (where $B_{c2} \equiv \mu_0 H_{c2}$). In addition, the flux-line—edge-surface interaction between the edge surface and a flux line is essentially magnetic

TABLE I. Properties of the amorphous samples.

Material	Sample	d (μm)	T_c (K)	ΔT_c (mK)	ρ_0 ($\mu\Omega$ m)	$-\mu_0 dH_{c2}/dT\,\|_{T_c}$ (T/K)	κ	$\xi(0)$ (nm)	$\lambda(0)$ (μm)	$B_c(0)$ (mT)
Nb_3Ge	176A	2.92	4.25	170	1.65	1.83	61	6.5	0.65	52
	175A	1.24	3.99	77	1.57	2.01	63	6.4	0.66	52
	174B	0.62	3.86	10	1.64	2.04	65	6.5	0.68	50
	191B	0.46	4.00	12	1.66	1.97	64	6.4	0.68	50
Mo_3Si	20B	0.46	7.69	130	1.48	1.86	59	4.8	0.46	99
Nb_3Si	27C	2.48	3.52	130	1.80[a]	2.02	67	6.8	0.74	44
	26A	0.96	3.19	22	1.80	1.85	64	7.5	0.78	38
	31B	0.71	3.36	45	1.80[a]	1.94	66	7.1	0.77	40
	29B	0.22	3.20	14	1.81	1.73	63	7.7	0.79	36

[a]Not measured; value for Nb_3Si 26A is assumed.

with characteristic range $\lambda \approx 1$ μm. Hence, the effect of small edge irregularities (size $\ll\lambda$) is averaged out over distances of order λ, whereas large irregularities do not contribute essentially to the pinning force. Recent experiments show that edge pinning due to cutting strips of amorphous MoRuB is considerably stronger than the pinning we encounter in our samples.[22]

Surface roughness may contribute largely when flux pinning is measured in a perpendicular field. It may cause FLD as well. Scanning electron microscopy did not reveal any surface irregularities, but this technique has a limited resolution of only 2–4 nm. Recently, however, Barbee and Keith[23] reported on thickness uniformity to tenths of angstrom units in sputter-deposited amorphous layers. The free-surface smoothness essentially replicates the smoothness of the substrates. Hence, the quality of the substrates is of essential importance. We used polished single-crystalline or polycrystalline sapphire substrates, the latter were selected for large, almost identically oriented grains. They all were cleaned very carefully before film deposition. From small-angle x-ray diffraction studies by Pomerantz and Segmüller[24] it is known that the surface roughness of similar substrates such as silicon and quartz is smaller than 1 Å. It is thought that the roughness is steplike and has a very low areal density, but no definite experimental evidence is available at present. In conclusion, we believe that sputter-deposited amorphous transition-metal superconductors on well polished and cleaned substrates are the best obtainable samples for the study of 2D collective pinning phenomena.

III. EXPERIMENTAL RESULTS AND DISCUSSION

An example of typical I-V curves is given for amorphous Nb_3Ge 191B at $t = T/T_c = 0.5$ in Fig. 1. The 1-μV criterion defining the critical current and current density I_c and J_c is denoted by the crosses. There clearly exists a transition region from zero voltage to linear voltage-current behavior known as the flux-flow regime. Therefore J_c cannot be sharply defined. It turned out, however, that the characteristic features we discuss in this section are not influenced by this ambiguity. The pinning force per unit volume is defined by $F_p = BJ_c$. Reduced pinning forces $F_p(b)/F_p(0.4)$ are plotted against the reduced magnetic induction in Figs. 2(a)–2(c), respectively, for Nb_3Ge 191B, Mo_3Si 20B, and Nb_3Si 29B at several temperatures. All the samples studied in this work display the same characteristics as those obtained for Nb_3Ge 176A, 175A, and 174B reported in I. Again, three regimes can be distinguished: $0.1 < b < b_{RN}$, $b_{RN} < b < b_p$, and $b_p < b < 1$, where b_{RN} is the field that marks the onset of the peak in $F_p(b)$ and b_p is defined by linear extrapolation as indicated by the dotted lines in Fig. 2(a).

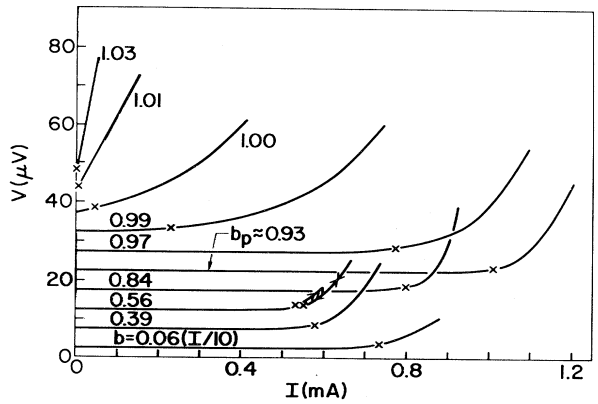

FIG. 1. Representative examples of I-V curves (recorder traces) for Nb_3Ge 191B at $t = 0.5$. The curves are labeled by the reduced field values $b = B/B_{c2}$ at which they were recorded. Every curve is shifted by a vertical voltage offset. For $b = 0.06$ the I is divided by 10. At $b = 0.56$ FLL rearrangement at low velocities is observed. The crosses denote the 1-μV criterion for I_c.

A. The region below b_{RN}

The solid and dashed lines in Figs. 2(a) and 2(b) represent the evaluation of the data in terms of the 2D LO theory using Eqs. (B11) and (B12) together with Brandt's expression for c_{66} in the large κ limit[26]:

$$c_{66} = \frac{B_c^2(t)}{4\mu_0}\frac{\kappa^2}{\kappa_2^2} b(1-0.29b)(1-b)^2 . \quad (1)$$

Since we do not know *a priori* what causes the pinning in our samples we inserted for $W(0)$ the two possible relations related to reasonably well-established forms for $f_p(b)$, namely[7,8]

$$W(0) = C_n(t) b^n (1-b)^2 \quad (2)$$

with either $n = 1$ or 3. For both cases $W(0)$ was adapted at $b = 0.4$. It is clear from Figs. 2(a) and 2(b) that below b_{RN} the case $n = 1$ gives excellent agreement with experiment, whereas $n = 3$ deviates for all fields. As follows from Fig. 2(c), the agreement for Nb_3Si is less satisfactory which we were able to attribute to the contribution of more than one predominant pinning mechanism. In this case $W(0)$ is given by

$$W(0) = (C_1 b + C_2 b^2)(1-b)^2 . \quad (3)$$

A detailed discussion of this and related phenomena (influence of H doping, for instance) is planned to be the subject of a forthcoming paper.

Confirmation of the 2D character independent of the origin of the pinning is provided by a plot of $F_p(b = 0.4, t = 0.7)/B_c^2(0.7)$ vs d^{-1}, as shown in Fig. 3. The results for Nb_3Ge agree very well with the expectation $F_p \propto d^{-1}$ [Eq. (B16)]. Again, the results for the Nb_3Si samples deviate from this prediction, although the general trend is observed. The larger fluctuations from sample to sample suggest the Nb_3Si samples were less consistently prepared than the Nb_3Ge specimens, which have very good comparable characteristics. We should note here that pinning by surface roughness alone[22] would also result in $F_p \propto d^{-1}$, but only if $d \gg \lambda$, which does not apply for our samples. Besides, one must assume a very rough surface structure to explain the magnitude of F_p. Therefore it is ruled out as a possible source of flux pinning in our specimens, but it might be of importance for splat-cooled amorphous su-

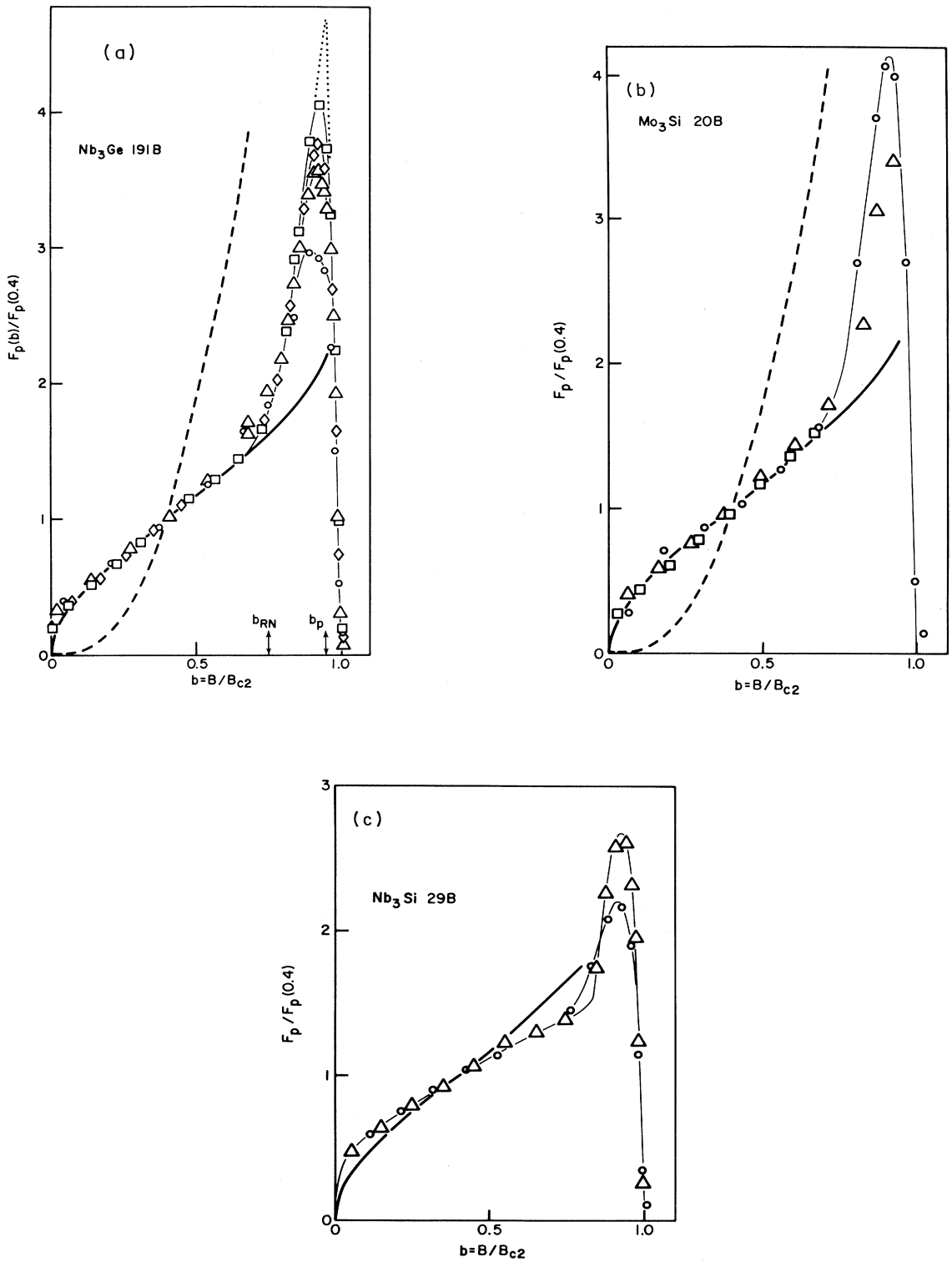

FIG. 2. Normalized volume pinning force vs b. (a) Nb_3Ge 191B at $t=0.79$ (circles), $t=0.70$ (triangles), $t=0.50$ (squares), and $t=0.40$ (diamonds). The solid and dashed lines represent the 2D LO theory with $W(0)=C_n(t)b^n(1-b)^2$ with $n=1$ and 3, respectively. The other lines are guides for the eye. The dotted straight lines are extrapolations to define b_p. The field at which the data start to deviate from the solid line is defined as b_{RN}. (b) Same for Mo_3Si 20B at $t=0.75$ (circles), $t=0.50$ (triangles), and $t=0.25$ (squares). In the latter cases B_{c2} could not be measured and therefore was obtained from $-\mu_0 dH_{c2}/dT\,|_{T_c}$ and the dirty-limit Ginzburg-Landau- A'brokosov-Gor'kov (GLAG) theory.[25] (c) Same for Nb_3Si 29B at $t=0.80$ (circles) and $t=0.60$ (triangles). In this case only the case $n=1$ is depicted. It does not give a good fit due to the contribution of more than one pinning mechanism.

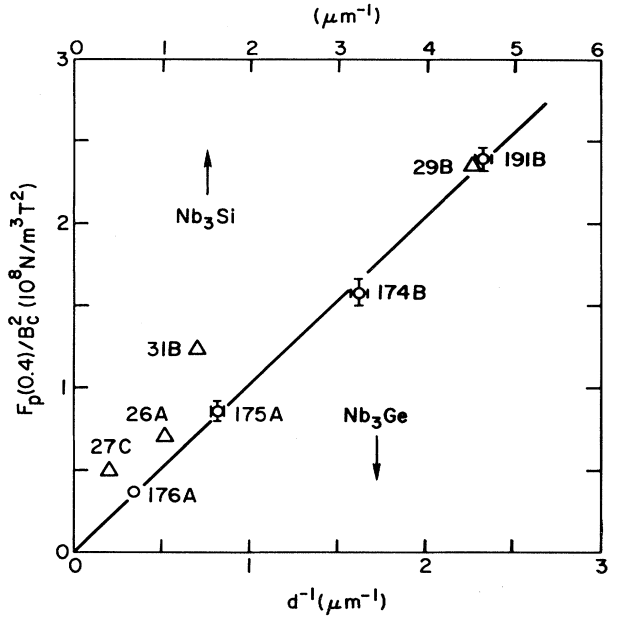

FIG. 3. Plot of F_p/B_c^2 vs d^{-1} at $b=0.4$ and $t=0.7$ for Nb_3Ge (circles) and $t=0.65$ for Nb_3Si (triangles). The division by $B_c^2(t)$ accounts for most of the small variations in the superconducting parameters of the samples, like T_c and $B_c(0)$.

perconductors.[22]

More insight into the experimental results can be obtained by assuming the 2D LO theory describes the flux pinning, so that $W(0)$ and R_c can be computed from the data. The temperature and field dependences of $W(0)$ provide valuable information about the defect character of our amorphous superconductors, which will be dealt with in the next section. The relative size of the correlated regions R_c/a_0 as a function of b is depicted for $b<b_{RN}$ by the open symbols in Fig. 4. We observe a strikingly uniform behavior irrespective of temperature or material. According to Eq. (B18) R_c/a_0 is inversely proportional to the relative displacement per flux line and therefore the data in Fig. 4 roughly reflect the functional dependence of the shear modulus on b [Eq. (1)] depicted by the dashed line. It demonstrates the increase of positional disorder with decreasing c_{66} for both small and large values of b.

B. The region of the peak

It is observed that for all samples and temperatures the peak starts to come up at values of $R_c/a_0 \approx 15-20$ at $b=b_{RN}\sim 0.7-0.8$. Because it is well established that in highly disordered solids and glasses the elastic moduli are softened with respect to the ordered state,[27,15,18] we suggested in I that the peak is caused by softening of the shear modulus due to the increasing disorder. Within the framework of the 2D LO theory one other possible explanation is that $W(0)$ increases in the peak region, but in the case of small defects ($\lesssim\xi$) there is no reason to expect changes in the long-wavelength behavior of the pinning correlation function with increasing disorder.[3] Therefore we discard this possibility and assume that $W(0)$ for

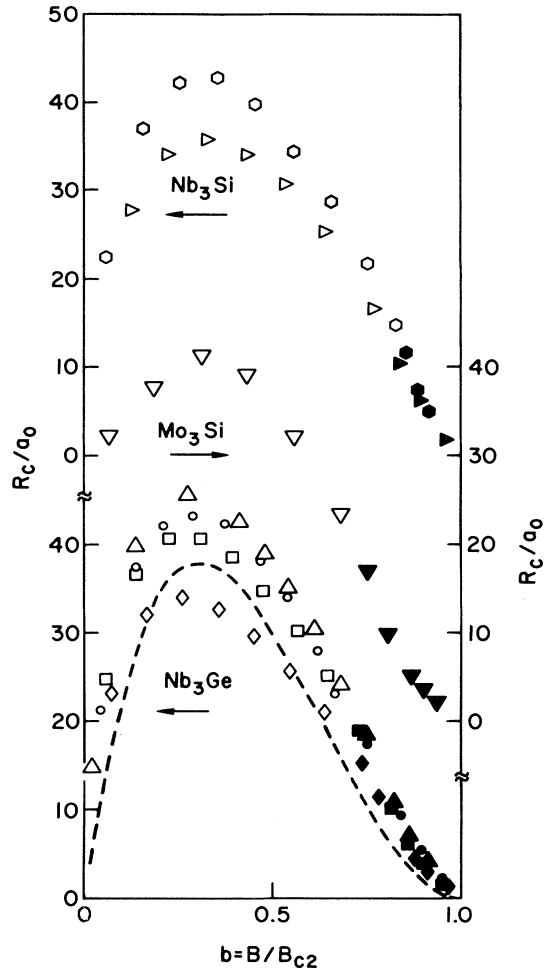

FIG. 4. Correlation length R_c relative to a_0 plotted vs b. Data for Nb_3Ge 191B at $t=0.79$ (circles), $t=0.70$ (triangles), $t=0.50$ (squares), $t=0.40$ (diamonds), for Mo_3Si 20B (note the shift in vertical scale) at $T=0.75$ (inverted triangles); for Nb_3Si 29(B) at $t=0.80$ (canted triangles) and $t=0.60$ (hexagons). Open symbols refer to the region below the peak in which the 2D LO theory holds with c_{66} from Eq. (1); filled symbols refer to the region of the peak in which c_{66} is reduced due to pinning renormalization. The field dependence of c_{66} (in arbitrary units) as given by Eq. (1), is depicted by the dashed line.

$b_{RN}<b<b_p$ is given by its extrapolation from the field range below b_{RN}. In the cases of Nb_3Ge and Mo_3Si this is simply described by Eq. (2) with $n=1$. For Nb_3Si we used Eq. (3). From Eqs. (B13) and (B14) the renormalized shear modulus $\tilde{c}_{66}$ as well as R_c/a_0 can then be obtained by substitution of the experimental F_p's. In Fig. 4 the data determined in this way are depicted by the filled symbols. We note that approaching $b=b_p$ the values of R_c reduce to $1-2a_0$, which means that the FLL has become amorphous at and beyond b_p.

The reduction of the shear modulus with increasing disorder is displayed by a plot of $\tilde{c}_{66}/c_{66}$ vs $(R_c/a_0)^{-1}$ as shown in Fig. 5 for the samples discussed in this paper. In Fig. 6 the results at $t=0.7$ of the four Nb_3Ge samples with $d=0.46$, 0.62, 1.2, and 2.9 μm can be compared.

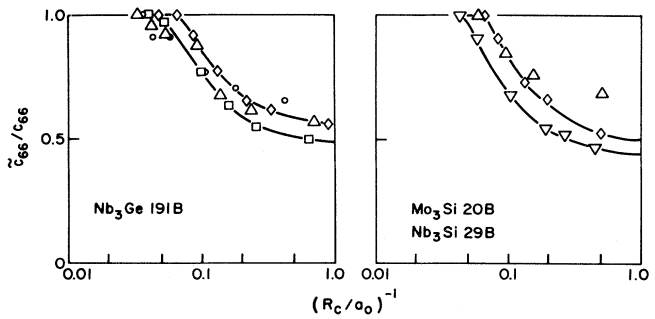

FIG. 5. Renormalized $\tilde{c}_{66}$ relative to the value for a perfect FLL vs $(R_c/a_0)^{-1}$ displaying the amount of disorder in the FLL. Same samples and symbols as in Fig. 4 except for Nb_3Si: $t=0.80$(△) and $t=0.60$ (◇). The lines are guides for the eye.

Three features can be deduced from these figures. The reduction sets in very sharply and levels off at values between 10% and 50%. There is no clear correlation with temperature, but there seems to be a relation between the thickness and the ultimate values of $\tilde{c}_{66}/c_{66}$.

In the onset region of the peak, corresponding to the field range where $\tilde{c}_{66}/c_{66}$ drops sharply, we often observed instabilities in the I-V curves at low voltage level. A typical example is shown in Fig. 1 for $b=0.56$. When the current ramp is interrupted, the voltage decreases gradually with time, approximately proportional to $\exp(-t/\tau)$ with $\tau\sim 7.5$ s, to a limiting value that reproduced on reversal of the current ramp. Possibly, the FLL, when it is moving with small velocity, is able to adjust itself better to the random pinning field, thereby reducing the average size of the correlated regions and hence the average value of $\tilde{c}_{66}$. This avalanching process emerges until a dynamic equilibrium is attained. At higher values of b this phenomenon disappears in agreement with the leveling off of the decrease in $\tilde{c}_{66}/c_{66}$ for $R_c \leq 5a_0$.

A crossover from a two-dimensional to a three-dimensional collective pinning regime should be considered as a possible mechanism for the peak effect. We

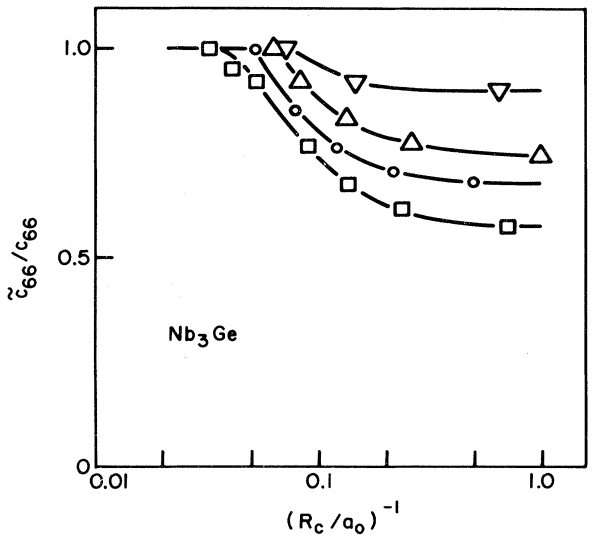

FIG. 6. Plot of $\tilde{c}_{66}/c_{66}$ vs $(R_c/a_0)^{-1}$ for the Nb_3Ge samples at $t=0.7$: 176A (inverted triangles), 175A (triangles), 174B (circles), and 191B (squares).

note that the three-dimensional collective-pinning theory predicts an exponential decrease of R_c and L_c, due to the dispersion of the elastic modulus c_{44} near $b=1$. If the 2D-3D transition occurs when $L_c \approx d$, it should occur at higher fields for thinner samples. However, as seen from Table II, the opposite is observed. Namely, b_{RN} increases with thickness. Another argument against this mechanism is provided by the fact that R_c and L_c as determined from the 3D collective pinning expressions are, for all fields, about 4 orders of magnitude larger than those obtained from the 2D theory for R_c and Eq. (10) for L_c.

C. The region above the peak

For fields larger than b_p the flux lines are optimally adapted to the randomly distributed pinning centers. Therefore R_c/a_0 is a constant in the field range $b_p < b < 1$.

TABLE II. Comparison of the 2D melting field computed from Eq. (6) for two values of the renormalization parameter A_2 with the experimentally determined fields b_{RN} and b_p of the Nb_3Ge samples.

Sample Nb_3Ge	T (K)	$(1-b_m)$ $A_2=0.5$	$(1-b_m)$ $A_2=1.0$	$(1-b_{RN})$	$(1-b_p)$
191B	3.16	0.177	0.125	0.28	0.10
	2.78	0.147	0.104	0.25	0.08
	2.00	0.109	0.077	0.24	0.07
	1.60	0.095	0.067	0.24	0.07
174B	3.48	0.223	0.158	0.25	0.07
	2.71	0.129	0.091	0.18	0.05
	1.93	0.094	0.066	0.18	0.04
175A	3.58	0.148	0.105	0.16	0.025
	2.80	0.089	0.063	0.12	0.03
	2.00	0.065	0.046	0.15	0.025
176A	2.99	0.058	0.041	0.10	0.015

For this amorphous FL structure the 2D theory predicts

$$F_p=[W(0)/dR_c^2(b_p)]^{1/2}\ , \tag{4}$$

which agrees with the linear decrease $\propto(1-b)$ we observed in all cases. There is no correlation found between the nonuniformity of the samples, of which ΔT_c in Table I is an appropriate measure, and the widths of the field region in which F_p drops to zero. However, with larger ΔT_c more rounding is observed at $b\approx b_p$ and $b\approx 1$, which can be understood in terms of a larger nonuniformity. The sharpness of the drop itself is not affected. This feature provides us with a check on the prefactor $C_n(t)$ in Eq. (2). As will be discussed in Sec. IV, satisfactory agreement is found for $n=1$. Therefore, the conclusion so far is that all phenomena observed in our samples self-consistently demonstrate the 2D collective pinning behavior. In most cases the pinning is governed by the parameter $W(0)$ as given in Eq. (2) with $n=1$, in some cases we obtain a better agreement by assuming a second pinning mechanism so that $W(0)$ is given by Eq. (3).

D. The region $b\gtrsim 0$

Not much is known about the pinning behavior for very small fields where the flux lines are well separated. Since c_{66} goes to zero in this region, R_c/a_0 tends to decrease with decreasing fields as seen in Fig. 4. It is expected[2] that eventually the FLL becomes amorphous, so that pinning is described by Eq. (4). Again $R_c\approx a_0$, but $W(0)$ is now essentially field independent.[8] This results in a pinning force $F_p\propto a_0^{-1}\propto\sqrt{b}$, which is experimentally observed, although we did not study this field region in great detail. Note that the critical current diverges as $J_c(b)\gtrsim\propto b^{-1/2}$.

E. Pinning enhancement H_{c2}: Lattice softening, melting, or thermal activation of disorder?

By assuming the softening of the shear modulus we were able to explain the pinning enhancement above $b_{\rm RN}$. Although the reduction we found for c_{66}, agrees in magnitude with reductions of 30—60 % obtained from computer simulation[15,27] for glassy solids, this result may be rather fortuitous because of the different dimensionality and the quite different nature of the interaction between flux lines, which is very long range, especially for thin films and for $b\rightarrow 1$. The effective range of the interaction[26,29,30] can be estimated by

$$\lambda_{\perp,\rm eff}(T,B,d)\approx\frac{\lambda(T)}{\sqrt{1-b}}\coth\left[\frac{d\sqrt{1-b}}{2\lambda(T)}\right]\ , \tag{5}$$

where $\lambda(T)$ is the weak-field penetration depth. At $b_{\rm RN}$, for example, $\lambda_{\perp,\rm eff}\approx 20R_c\approx 400a_0$. From Brandt's paper[26] on c_{66} one can conclude that the shear modulus, especially for $\kappa\gg 1$, is predominantly determined by the short-range attractive part of the model potential. There is, however, neither a quantitative agreement nor a correlation between this range and R_c at $b=b_{\rm RN}$. In a subsequent paper[11] Brandt predicts that the shear modulus for shearing of closest-packed planes decreases by more than 50% if the wave vector k of the periodic displacement field approaches the Brillouin zone at $2\pi/a_0\sqrt{3}$. For shearing perpendicular to this direction on the other hand, a large increase of the shear modulus is obtained. Very likely, the short-range order correlation length R_c is related to some characteristic wavelength of the displacement field. In addition, the FLL will conform itself to the distribution of the pinning centers in such a way as to yield the smallest increase in elastic energy. Hence, it will take as much advantage of the decrease of $c_{66}(k)$ as possible. Brandt's theoretical results, therefore, might support our view that the enhancement in the pinning is caused by a decrease of c_{66} for short-wavelength distortions. It is not clear, however, how this relates to the abruptness with which the reduction of c_{66} sets in, as is displayed in Figs. 5 and 6. This might be an indication that some other mechanism, related to a phase transition of the FLL is responsible.

The FLL in our samples form a 2D lattice in which, in case there is no flux pinning, one may expect to observe 2D phase transitions predicted by Kosterlitz and Thouless,[12] Our samples are too thick to satisfy the requirement[31] $\lambda_{\perp,\rm eff}\gtrsim w$, the width of the sample, so that the vortex-antivortex transition in zero field is experimentally not accessible for us. But we should be able to see the 2D melting transition that occurs when a fraction of the thermally excited dislocation pairs dissociate.[12,13] For a measuring temperature T, one obtains from Eq. (2.17) of Ref. 14 an expression for the reduced flux density b_m at which the melting transition should occur

$$(1-b_m)^2=0.5\frac{B_{c2}(T)T}{A_2B_c^2(T)d}\ . \tag{6}$$

The quantities d, B_c, and B_{c2} are measured in μm, mT, and T, respectively. A_2 is a parameter that accounts for the renormalization of the shear modulus due to the bound dislocation pairs. Its value is expected to lie between 0.4 and 1 and it is slightly dependent on the magnetic field.[14] In Table II the computed values of $(1-b_m)$ for $A_2=0.5$ and 1 are summarized and compared with the values of $(1-b_{\rm RN})$ and $(1-b_p)$ as measured for the Nb_3Ge samples. Here, b_p for Nb_3Ge 191B was somewhat differently defined as the field where the actually measured F_p is maximum. The only positive correlation is the order of magnitude agreement and the thickness dependence, although neither for $(1-b_{\rm RN})$ nor for $(1-b_p)$ the $d^{-1/2}$ behavior is found; both rather follow a d^{-1} dependence. The most obvious disagreement is the temperature dependence of the computed melting fields versus the nearly constant $b_{\rm RN}$'s and b_p's. Therefore, from the comparison of fields we cannot conclude in favor of a melting transition neither at $b_{\rm RN}$ nor at b_p. Moreover, as follows from Fig. 1, we could not detect any voltage rise well below the critical current for fields below and beyond $b_p=0.93$, even if the resolution was increased to 20 nV. In case of melting, the shear modulus should drop to zero leading to a flow of flux lines which we suppose to be detectable with our conventional measuring technique.

The reason we fail to find any convincing indication for melting must be the action of the pinning centers that give rise to correlated regions. If one visualizes these regions as differently oriented grains with a nearly perfect FLL inside, separated by grain boundaries, one can imagine

that the thermally excited dislocation pairs are not free to move throughout the entire sample, but are limited to the grains in which they were activated because of the action of the grain boundaries that leads to pinning of dislocations.[32] So, the interaction with the disordered boundaries of the correlated regions might prevent the detectable flow of flux lines. Recently, Fisher, Halperin, and Morf[33] pointed out that the melting criterion (in absence of pinning) is the same for grain boundary mediated melting. In the 2D collective pinning no account was taken of the decrease of free energy arising from the entropy related to the disorder. It, therefore, actually is a $T=0$ theory. In a simple attempt to combine collective pinning (equal to random field) with the thermal activation of grain boundaries we arrive at the following expression for the increase in free energy per unit volume[2,33] (see Appendix B for notation):

$$\delta F \approx \frac{\mu}{4}\left[\frac{a_0}{R_c}\right]^2 - \tfrac{1}{2}(W_a)^{1/2}\frac{a_0}{R_c} - \beta\frac{k_B T}{R_c^2}\frac{R_c}{a_0}, \tag{7}$$

where k_B is the Boltzmann constant and β is an adaptable parameter of the order 1 proportional to $(a_0/s)\ln(s/a_0)$, in which s is the spacing of the dislocations in the grain boundaries. Minimizing with respect to R_c yields a temperature-dependent correlation length

$$R_c = \frac{\mu a_0}{\beta k_B T/a_0^2 + (W_a)^{1/2}} . \tag{8}$$

Using

$$F_p = \frac{(W_a)^{1/2}}{dR_c} \tag{9}$$

and the requirement $W_a = dW(0) \propto b(1-b)^2$, one can eliminate W_a from Eq. (8) and obtain the proportionality constant of W_a as well as the parameter β in an iterative procedure carried out at two values of b, one at ≈ 0.25 far below b_{RN} and one close to $b=b_p$. In this way we got, for instance, an excellent fit of the entire $F_p(b)$ curve up to b_p for Nb_3Ge 191B at $t=0.7$ with $\beta=1.4$. Within 10% the same $W(0)$ and R_c/a_0 were retained for fields below b_{RN}. For $\mu = dc_{66}$ the nonrenormalized values of Eq. (1) were used. Applying the same routine with the same β of 1.4 at $t=0.4$ and for Nb_3Ge 176A at $t=0.7$ did not yield a very satisfactory result. We therefore do not want to claim that the mechanism expressed by Eq. (7) can universally explain the pinning behavior in our samples. We merely want to point out that no satisfactory theory exists today that combines the elements of collective pinning (random field) and the thermal activation of disorder (entropy term). An approach we attempted in this paragraph may eventually be justified by theory. From an experimental point of view it would be desirable to measure c_{66} as was done by Fiory[34] for granular Al films. Also, computer simulations will be of great use to check our assumption for the softening of the shear modulus.

F. Condition for 2D collective pinning

We are now in a position to derive the criterion to observe 2D collective pinning, namely $L_c \gg d$. An estimation of L_c is obtained by comparison with the 3D LO theory,[2,3] which suggests quite naturally

$$L_c \approx \left[\frac{c_{44}}{c_{66}}\right]^{1/2} R_c \approx 3\kappa\frac{(b)^{1/2}}{1-b}R_c . \tag{10}$$

Since $R_c \propto (1-b)$ and $R_c \gtrsim 2\ \mu$m at $b=0.1$, $L_c \gtrsim 100\ \mu$m, much larger than the thicknesses of our samples. In order to translate the condition $L_c \gg d$ in direct accessible quantities, we present

$$J_c^{1/2} \ll 0.2 B^{1/4} d^{-1} \tag{11}$$

with J_c in A/m^2, B in T, and d in m. In most cases $B^{1/4} \approx 1$, so that for pinning systems with $J_c \sim 10^9$ A/m^2 the samples must be much thinner than 6 μm. For amorphous superconductors J_c's of $\sim 10^5$ A/m^2 are reported[35] leading to $d \ll 600\ \mu$m. But it should be pointed out again, that a smooth surface and $\kappa \gg 1$ are important conditions as well (Sec. II).

IV. THE PINNING FORCE IN TRANSITION-METAL GLASSES

As in crystalline materials flux pinning in superconducting metal glasses arises from interactions with defects.[36] The nature of defects in amorphous materials is still a subject of numerous investigations, mostly by computer modeling. The work of Srolovitz *et al.*[37] concentrates on structural defects as the regions in which the internal stresses and local symmetry coefficients on an atomic scale deviate significantly from their average value. The work of Chaudhari *et al.*[38,15] is devoted to stability computations of larger scale defects such as edge and screw dislocations, vacancy clusters, and dislocation loops. The conclusion of these recent studies is that all of these defects are stable at zero temperature. Kronmüller *et al.*[16,39] were able to describe the magnetic saturation of amorphous ferromagnets by proposing clusters of quasi-dislocation dipoles as the predominant defect structure. For sputter-deposited films we rather think of quasidislocation loops, with the plane of the loop parallel to the plane of the film, as the defects responsible for flux pinning. But we also should consider inclusions of sputter gas, though they are supposed to be very small (of atomic size) and for alloys it might be that the fluctuations in composition and/or chemical order (microcrystallites, comparable to precipitates in crystalline substances) contribute to the pinning. As in the case of domain wall pinning in ferromagnets,[39] we expect that only the more extended dislocation loops [of sizes comparable to $\xi(0)$] can give a reasonable contribution to the pinning force. As to the microcrystallites, we know they were not detectable with the TEM analysis nor with x rays, which limits their size to less than 1 nm and their volume density to at most 1%.

For dislocation loops, vacancies, and precipitates reasonably well-established expressions for the elementary pinning force f_p are available in the literature. The first-order elastic interaction (volume effect) of a dislocation loop with diameter D has been derived by Pande[40] and Kramer.[41] For $D \ll a_0$ it is given by

$$f_{p,\mathrm{dl}} \approx \frac{2\pi^2}{9} C(1-b) D^2 b_0/a_0 \tag{12a}$$

hence

$$W_{\rm dl}(0)\approx C_{\rm dl}(t)b(1-b)^2 . \tag{12b}$$

Here b_0 is the Burgers vector and $C=\mu(1+v)\delta\epsilon_{v0}/(1-\nu)$ with μ the shear modulus and ν the Poisson ratio of the superconductor. The volume dilatation $\delta\epsilon_{v0}$ can be related to the pressure dependence of B_c by[42] $\delta\epsilon_{v0}=(B_c/2\mu_0)\times dB_c/dp$ leading to

$$C_{\rm dl}(t)\propto n_v D^4 B_{c2}(t)B_c^2(t)\left[\frac{dB_c}{dp}\right]^2 . \tag{13}$$

This $C_{\rm dl}(t)$ is equivalent to $C_l(t)$ in the preceding section. We do not take into account the second-order elastic interaction of a dislocation loop here, although it has been reported[9,36,43] to be somewhat larger, but it essentially has the same dependences on loop diameter, field, and temperature. It should be noted that any numerical result we obtain from the following analysis is only a rough estimate.

The expression for the elementary interaction of vacancies or voids of volume D^3 has been derived by Campbell and Evetts[7] and Kramer[8]

$$f_{p,\rm vac}\approx\left[\frac{2\pi}{a_0}\right]^3\xi^2(1-b)D^3B_c^2/\mu_0 \tag{14a}$$

which results in

$$W_{\rm vac}(0)\approx C_{\rm vac}(t)b^3(1-b)^2 , \tag{14b}$$

where $C_{\rm vac}(t)=C_3(t)$ in Sec. III.

For small precipitates Kramer and Freyhardt[44] showed that $f_{p,\rm prec}$ is considerably smaller than $f_{p,\rm vac}$, roughly by a factor $(D/\xi)^2$. In a forthcoming paper we plan to discuss the elementary interaction of vacancies and precipitates more extensively, taking into account some doubt that has been raised[2,10] about the validity of Eq. (14a). As a matter of fact, Thuneberg *et al.*[45] very recently pointed out that D^3 should be replaced by $D^2\xi_0$ or by (Ref. 10) $D^2\xi(0)$. For the discussion here it suffices to point out that the interaction with precipitates and vacancies leads to a $b^3(1-b)^2$ field dependence of $W(0)$ [Eq. (14b)]. In Sec. III (Fig. 2) we demonstrated that this behavior is not observed in any of our samples. In addition, a quantitative analysis shows that we have to assume either much larger defect sizes or much larger densities than the limiting values set by the TEM observations, in order to account for the experimental value of $W(0)$ at $b=0.4$. For example, assuming a vacancy diameter of 0.3 nm, a density is required so large that the mutual distance of the vacancies should be 0.3 nm as well, which makes no sense at all.

As was noted in Sec. III, the best way of analyzing the pinning characteristics is provided by a plot of $W(0)/(1-b)^2$ vs b as given in Fig. 7 below the peak region. For Nb_3Ge and Mo_3Si $C_{\rm dl}(t)$ is determined from the slope of the straight lines through all the data points, for Nb_3Si only the data below $b\approx0.5$ were considered. For $t\approx0.7$ the resulting values of $C_{\rm dl}$ are listed in Table III. These can be directly compared to the values we obtained from the linear behavior above $b=b_p$ as discussed in Sec. III C. Taking into account the experimental accuracy one

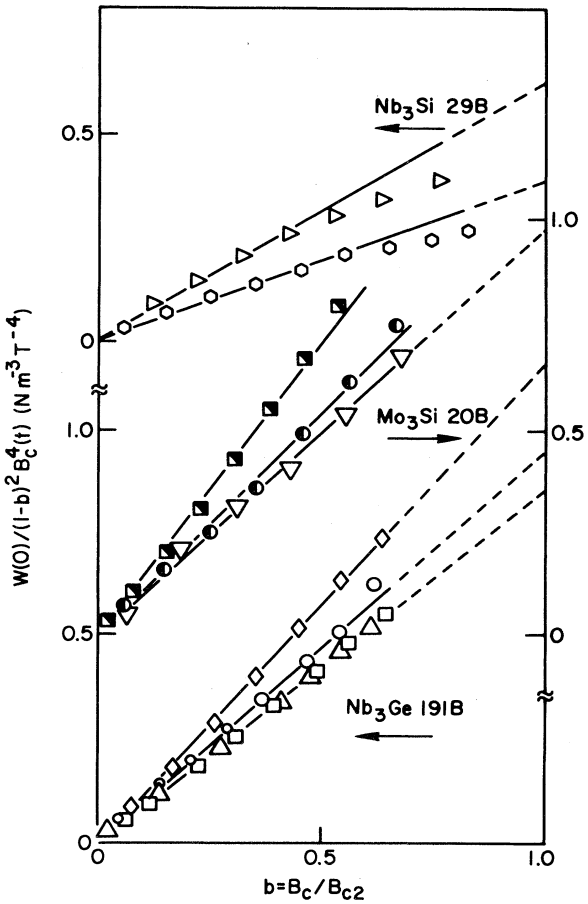

FIG. 7. Plot of $W(0)/(1-b)^2B_c^4(t)$ vs b as obtained from F_p vs b (Fig. 2) and Eqs. (B13) and (B14). Results for Nb_3Ge 191B at $t=0.79$ (circles), $t=0.70$ (triangles), $t=0.50$ (squares), $t=0.40$ (diamonds); for Mo_3Si 20B at $t=0.75$ (inverted triangles), $t=0.50$ (half-filled circles), $t=0.25$ (half-filled squares); for Nb_3Si 29B at $t=0.80$ (canted triangles) and $t=0.60$ (hexagons).

may conclude that the correspondence is very satisfactory.

In order to compare the characteristics for the different samples, we prefer to look at $C_{\rm dl}/B_c^2B_{c2}^2$, because this absorbs most of the temperature dependence (the data were sometimes taken at slightly different reduced temperatures) and the small differences in the superconducting properties of samples of the same material. The quantity dB_c/dp in Eq. (13) plays a minor role, since it has been empirically established by Rohrer[46] that it is roughly proportional to $(1+at^2)$, where the constant a can be either positive or negative, but it always turned out to be[46] much less than 1. The fact that for all three materials studied, almost the same value of $C_{\rm dl}/B_c^2B_{c2}$ is found (see Table III), points out the equivalency of the pinning mechanism and the density and size of the quasidislocation loops. Here we assume that quantities such as b_0, μ, ν, and dB_c/dp are almost equivalent for the different materials. For instance, for Nb_3Ge, adapting values observed for Nb, $b_0=2.8\times10^{-10}$ m, $\mu=3\times10^{10}$ N/m^2, $\nu=0.39$, and (Alers and Waldorf[47]) $\delta\epsilon_{v0}(t=0.7)\approx5\times10^{-8}$, we obtain

TABLE III. Characteristics of dislocation loop pinning at $t \approx 0.7$.

Sample		t	$C_{dl}(t)$ (10^{-7} N^2/m^3)	$C_{dl}(b > b_p)$ (10^{-7} N^2/m^3)	$C_{dl}/B_c^2 B_{c2}$ (10^{-4} N^2/m^3 T^3)
Nb_3Ge	176A	0.70	4.6	6.8	2.7
	175A	0.70	4.3	3.9	2.4
	174B	0.70	3.0	3.1	1.9
	191B	0.70	3.8	3.4	2.3
Mo_3Si	20B	0.75	33	14	5.0
Nb_3Si	27C	0.71	2.5	3.8	2.6
	26A	0.65	1.3	2.7	1.3
	31B	0.60	2.7	2.5	1.6
	29B	0.60	1.1	0.5	0.93

$n_v D^4 \approx 2 \times 10^{-10}$ m, which is a quite acceptable result. For example, assuming $D = 5$ nm [$\xi(0) \approx 7$ nm], we get $n_v \approx 3 \times 10^{23}$ m^{-3}, hence, an average spacing of 15 nm. For $D = 10$ nm, we obtain, respectively, 2×10^{22} m^{-3} and 37 nm. Very small loops, $D = 1$ nm, yield an unreasonable large density, $n_v = 2 \times 10^{26}$ m^{-3}, and, therefore, a very small spacing of 2 nm. A plot of $(C_{dl}/B_c^2 B_{c2})^{1/2}$ vs t^2, as displayed in Fig. 8, reflects the temperature dependence of dB_c/dp. The reasonable agreement with the linear expectation,[46] confirms the preceding conclusion that quasi-dislocation loops of size $\xi(0)$ are responsible for the flux pinning in the amorphous superconductors investigated.

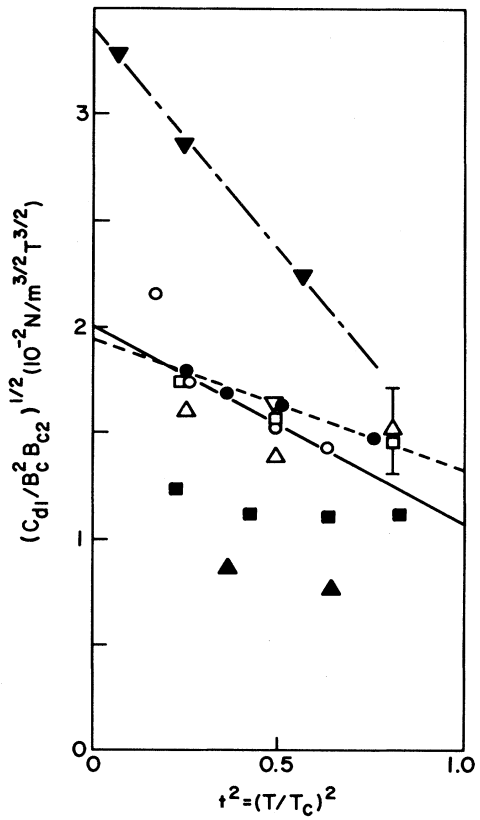

FIG. 8. Plot of $(C_{dl}/B_c^2 B_{c2})^{1/2} \propto dB_c/dp$ vs t^2 for Nb_3Ge 191B (circles), 174B (triangles), 175A (squares), 176A (inverted triangle), for Mo_3Si 20B (filled inverted triangles), for Nb_3Si 27C (filled circles), 26C (filled squares), and 29B (filled triangles).

V. STRUCTURAL RELAXATION

Structural relaxation studies of glasses provide unique insight in the dynamics and stability of the stress modulation on an atomic scale under thermal annealing at temperatures below the glass temperature.[37,48,17] Not much is known yet about the influence of structural relaxation on

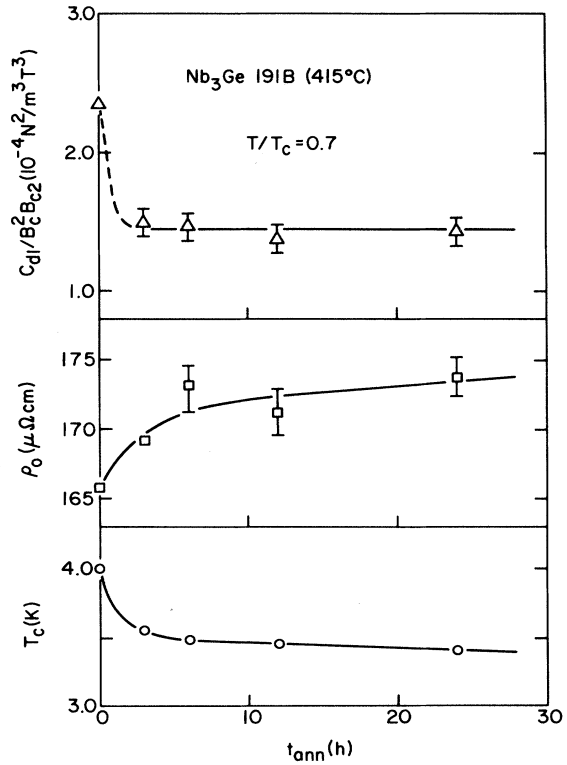

FIG. 9. Effect of structural relaxation on the (superconducting) properties of amorphous Nb_3Ge 191B after annealing at 415 °C for increasing annealing times t_{ann}.

TABLE IV. Superconductive properties of Nb_3Ge 191B and 175A before and after annealing at 415 °C and 580 °C, respectively. The data in the last three columns are taken at $t \approx 0.7$.

Sample Nb_3Ge	t_{ann} (h)	T_c (K)	ΔT_c (mK)	ρ_0 ($\mu\Omega$ cm)	$B_c(0)$ (mT)	$F_p(b=0.4)$ (10^4 N/m^3)	C_{dl} (10^{-8} N^2/m^3)	$C_{dl}/B_c^2B_{c2}$ (10^{-4} N^2/m^{3}T^3)
191B	0	3.998	12	166	50	16.1	38	2.3
	3	3.548	13	169	45	8.60	17	1.5
	6	3.478	13	174	43	7.67	14	1.5
	12	3.451	19	171	42	6.90	13	1.4
	24	3.400	20	174	41	7.40	14	1.4
175A	0	3.99	77	157	52	6.49	43	2.4
	24	3.25	17	164	41	3.39	17	1.3
	48	3.14	17	166	39	3.01	15	1.2

the more extended defects. In view of the results of the preceding section flux pinning is very likely to be a sensitive tool to obtain this information. In order to demonstrate this and as a prelude to more extensive investigations, we sequentially annealed sample Nb_3Ge 191B at 415 °C ($\ll T_{glass} \sim 750$ °C) for 3, 3, 6, and 12 h in a flow of purified He gas and studied the superconductive properties after each annealing treatment.

The results are summarized in Table IV and Figs. 9–11. Obviously, from Fig. 9, the most drastic changes take place within the first 3 h. Upon the first annealing step a much smaller but monotonous change in T_c and ρ_0 persists, whereas $F_p(0.4)$ and so C_{dl} seems to have been fully relaxed to a lower bound. Figure 10 shows a logarithmic decrease of T_c with t_{ann} as commonly observed[49,50] in glassy superconductors. This time dependence, as pointed out by Elmquist and Poon,[50] reveals a relaxation of internal strains characterized by a distribution in activation energy $f(E)$ and an attempt frequency proportional to $\exp(-E/k_BT)$, as observed in many physical systems. However, the mechanism leading to the decrease in T_c might be more complex than the phonon hardening model, adapted by these authors, which only seems to affect the denominator in the McMillan[51] formula for the coupling parameter $\lambda = N(0)\langle I^2\rangle / M\langle\omega^2\rangle$, whereas the increase of the resistivity we observed, indicates a decrease in $N(0)$. Additionally, there exists a density-of-states distribution related to the local-density fluctuations, which sharpens up after relaxation. Supposing T_c is determined by the maximum $N(0)$ in a volume ξ^3, this sharpening might also contribute to the change in T_c. All these effects are rather small (only several percent) and

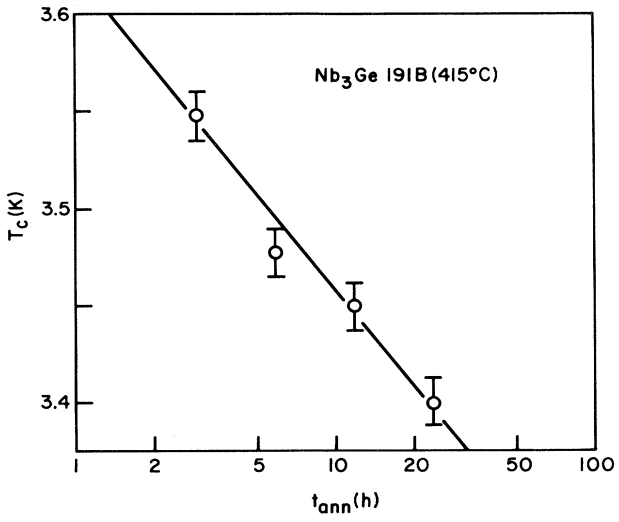

FIG. 10. Semilogarithmic plot of T_c vs annealing time for Nb_3Ge 191B (415 °C).

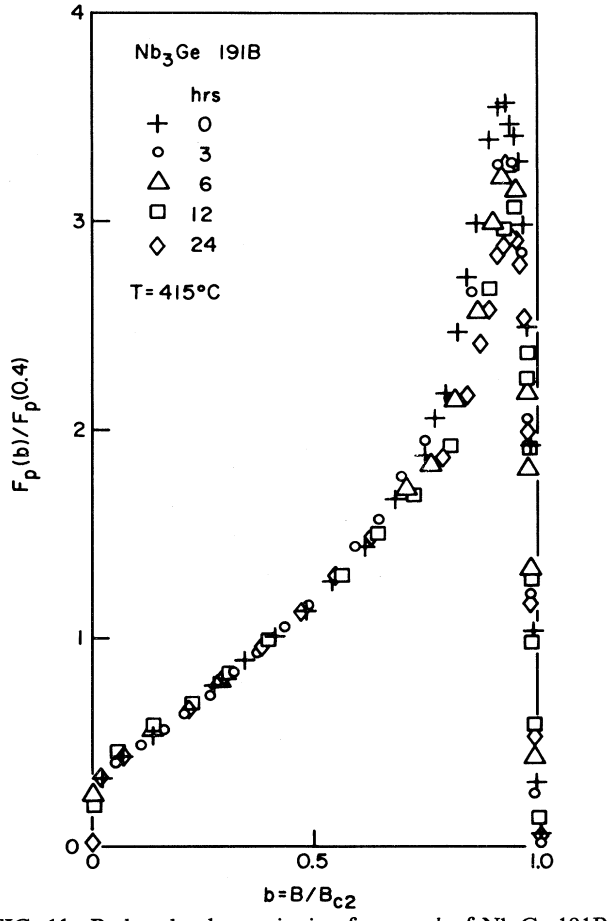

FIG. 11. Reduced volume pinning force vs b of Nb_3Ge 191B at $t = 0.7$ before (crosses) and after annealing for 3 h (circles), 6 h (triangles), 12 h (squares), and 24 h (diamonds).

may partially cancel each other. Therefore, it is hard to relate the change in T_c to only one of these, unless more experimental evidence is available. It is, however, rather well established that these changes are related to structural relaxations on an atomic scale.

Figure 11 shows very convincingly that the pinning characteristics do not change upon annealing. Also, plots of $W(0)/(1-b)^2$ vs b retain the linear behavior leading to the conclusion that dislocation loops still are the predominant pinning centers. The reduction of C_{dl} by a factor 1.5 points to a decrease of the average loop size by only 11%. This clearly demonstrates for the first time that extended defects in amorphous materials can be stable against thermal treatment well below the glass transition. It would be of interest to study the stability also as a function of the annealing temperature. Preliminary experiments on Nb_3Ge (annealed at 580 °C for 24 h) also reveal interesting results. Characteristic data are also listed in Table IV. The same features were observed as was the case for Nb_3Ge 191B. This leads us to the conclusion that annealing up to ~ 600 °C does not alter the characteristics of the extended defect structure.

ACKNOWLEDGMENTS

We wish to thank Y. Imry and P. Horn for stimulating conversations. P. Leary, H. Brodsky, and L. Attanasio are gratefully acknowledged for their preparation of the samples, E. Allessandrini for the TEM analysis. One of us (P. H. K.) wishes to thank IBM World Trade that made his stay at Thomas J. Watson Research Center possible.

APPENDIX A: EXPRESSIONS FOR SUPERCONDUCTOR PARAMETERS

In the case of weak-coupling amorphous superconductors the dirty-limit expressions as derived by Gor'kov[52] neglecting band-structure complication are supposed to hold relatively well. For the slope of H_{c2} vs T at T_c,

$$S \equiv -\mu_0 \left. \frac{dH_{c2}}{dT} \right|_{T_c} = \frac{8k_B}{2\pi eD} , \tag{A1}$$

where μ_0 is the magnetic permeability in vacuum, e is the elementary charge, and k_B is the Boltzmann constant. D is the electron diffusion coefficient, related to the electron mean free path l, the Fermi velocity v_F^*, and the density of states (per spin) at the Fermi level $N^*(0)$ (the asterisk denotes renormalized quantities[53]) by

$$D = \tfrac{1}{3} v_F^* l = [2e^2 \rho_0 N^*(0)]^{-1} . \tag{A2}$$

Using the Bardeen-Cooper-Schrieffer (BCS) expressions[54]

$$\tfrac{1}{2}\mu_0 H_c^2(0) = \tfrac{1}{2} N^*(0) \Delta^2(0) = 1.56 N^*(0) k_B^2 T_c^2 \tag{A3}$$

and

$$-\mu_0 \left. \frac{dH_c}{dT} \right|_{T_c} = 1.73 \mu_0 \frac{H_c(0)}{T_c} \tag{A4}$$

and the definition

$$\kappa = \tfrac{1}{2}\sqrt{2} \left. \left(\frac{dH_{C2}}{dT} \Big/ \frac{dH_c}{dT} \right) \right|_{T_c} , \tag{A5}$$

the following relations are obtained (all quantities in Système International (SI) units: $[\rho_0] = \Omega\,\mathrm{m}$, $[S] = \mathrm{T\,K^{-1}}$):

$$\kappa = 3.54 \times 10^4 [\rho_0 S]^{1/2} , \tag{A6}$$

$$\mu_0 H_c(0) = S T_c / 2.45\kappa , \tag{A7}$$

in units of T,

$$N^*(0) = 1.78 \times 10^{41} S/\rho_0 , \tag{A8}$$

in states $J^{-1}\,\mathrm{m}^{-3}\,\mathrm{spin}^{-1}$. From

$$\xi(T) = 0.85(\xi_0 l)^{1/2} \left(\frac{T_c}{T_c - T} \right)^{1/2} \equiv \xi(0) \left(\frac{T_c}{T_c - T} \right)^{1/2} \tag{A9}$$

[ξ_0 is the BCS coherence length $\hbar v_F^* / \pi \Delta(0)$] it follows

$$\xi(0) = 1.81 \times 10^{-8} [T_c S]^{-1/2} , \tag{A10}$$

in units of m. Note that $\xi(0)$ differs from the Ginzburg-Landau (GL) coherence length at $T = 0$, which is given by $\xi_{GL}(0) = [\Phi_0 / 2\pi\mu_0 H_{c2}(0)]^{1/2}$, $\Phi_0 = h/2e$ is the flux quantum. Finally, from Ref. 54, pp. 80 and 114,

$$\lambda(0) = \lambda_L(0)[\xi_0 / l]^{1/2} \tag{A11}$$

and

$$\kappa = 0.715 \lambda_L(0)/l \tag{A12}$$

[$\lambda_L(0)$ is the London penetration depth], we obtain, in units of m,

$$\lambda(0) = 1.63\kappa\xi(0) = 1.05 \times 10^{-3} (\rho_0 / T_c)^{1/2} . \tag{A13}$$

APPENDIX B: EXPRESSIONS FOR 2D COLLECTIVE PINNING

The average dimension of the correlated regions for the case of 2D collective pinning is given by dR_c^2, where d is the thickness of the sample and R_c is the correlation length over which short-range order persists in the (x,y) plane perpendicular to the magnetic field. An approximate expression for R_c can be readily obtained by a derivation similar to that given in Ref. 2, p. 410 (same notation):

$$R_c \approx a_0 d^{1/2} c_{66} / W(0)^{1/2} . \tag{B1}$$

However, Eq. (48) of Ref. 2 for the displacement correlation function has a logarithmic divergence for the 2D case, so that a more rigorous derivation of R_c seems desirable.

We start from the 2D displacement correlation function

$$\langle [\vec{u}(\vec{r}) - \vec{u}(\vec{0})]^2 \rangle = \frac{1}{d} \int \frac{d^2\vec{k}}{(2\pi)^2} \frac{W(\vec{k})(1 - \cos\vec{k}\cdot\vec{r})}{c_{66}^2 k^4} \tag{B2}$$

obtained from Eq. (48) of Ref. 2 by taking the limit $k_z \to 0$. Here $\vec{u}$ and $\vec{r}$ are vectors in the (x,y) plane denoting the displacement and the position of a flux line; $\vec{k}$ is the 2D wave vector of the displacement field. $W(\vec{k})$ is related to the correlation function of the inhomogeneities (pinning centers). As pointed out in Ref. 3 for distances $\rho = |\vec{r}| > a_0$, the small k values in (B2) are important. Therefore, the k dependence of W is neglected [$W(k) = W(0) + O(k^2)$ (Ref. 55)], and only

$$W(0) = n_v \langle f^2 \rangle \approx \tfrac{1}{2} n_v f_p^2 \tag{B3}$$

is retained, in which n_v denotes the number density of pinning centers. With the use of the definition

$$\vec{k} \cdot \vec{r} = |\vec{k}|\,|\vec{r}| \cos\phi_{\vec{k},\vec{r}} \equiv p \cos\phi_{\vec{k},\vec{r}} , \tag{B4}$$

Eq. (B2) yields

$$\langle [u(\rho) - u(0)]^2 \rangle = \frac{W(0)\rho^2}{4\pi^2 d c_{66}^2} \int_0^{2\pi} d\phi_{\vec{k},\vec{r}} \int_{p_1}^{p_u} dp \frac{1 - \cos(p \cos\phi_{\vec{k},\vec{r}})}{p^3} . \tag{B5}$$

The integration boundaries p_u and p_1 are related, respectively, to the Brillouin zone radius of the reciprocal[11] FLL and the largest wavelength of the displacement field that makes sense in a finite sample

$$p_u = \rho k_B = 2\sqrt{\pi}\rho / a_0 , \tag{B6a}$$

$$p_1 \approx \pi \rho / w , \tag{B6b}$$

where w is some suitable dimension of the sample, in our case the most proper choice seems to be the width. The result of the double integration in Eq. (B5) is[56] $G(p_u) - G(p_1)$ with

$$G(p) \equiv \pi \left[\frac{J_0(p) - 1}{p^2} - \frac{J_1(p)}{2p} - \frac{Ji_0(p)}{2} \right] , \tag{B7}$$

where $J_n(p)$ is a Bessel function of order n and

$$Ji_0(p) = \int_p^{\infty} dt\, J_0(t)/t .$$

Since $\rho \gtrsim a_0$ and thus $p_u \gtrsim 4$, it turns out[57] that $|G(p_u)| < 0.1$ for all relevant p_u and can be neglected. Because $p_1 \ll 1$ we obtain

$$G(p_1) = -\frac{\pi}{2}[1 - \gamma - \ln(p_1/2)] , \tag{B8}$$

where $\gamma = 0.5772$ is Euler's constant. So the final result is

$$\langle [u(\rho) - u(0)]^2 \rangle = \frac{W(0)\rho^2}{4 d c_{66}^2} X^{-1}(w/\rho) \tag{B9}$$

with

$$X(x) \equiv 2\pi / [\ln(x) - 0.029] . \tag{B10}$$

The quadratic dependence on ρ is to be expected for 2D systems with random fields.[4] It leads to a much faster growth of disorder than in 3D where it is only proportional to ρ. The logarithmic factor $X(w/\rho)$ is qualitative of minor importance.

The correlation length R_c is determined by the condition that $\langle [u(R_c) - u(0)]^2 \rangle^{1/2} \approx a_0/2$, which in view of the periodicity of the FLL is the range of the elementary pinning interaction, if the pinning centers are much less than a_0. Hence[1]

$$R_c = X^{1/2}(w/R_c)[a_0 d^{1/2} c_{66} / W(0)^{1/2}] . \tag{B11}$$

The volume pinning force is given by[2]

$$F_p = B J_c = [W(0)/d R_c^2]^{1/2} . \tag{B12}$$

Therefore $W(0)$ and R_c can be determined from F_p and

$$W(0) = X^{1/2}(w/R_c)(a_0 d c_{66} F_p) , \tag{B13}$$

$$R_c = X^{1/4}(w/R_c)(a_0 c_{66}/F_p)^{1/2} , \tag{B14}$$

which we used to evaluate our experimental data. As follows from a comparison of Eqs. (B1) and (B11), the size effect only enters logarithmically and, additionally, turns out to give for our experimental situation contributions of order $1 - 0.5$. Therefore, it is almost ignorable in comparison to the other approximations of the theory.[2,3]

Physically more transparent relations are obtained by introducing 2D quantities

$$\mu = d c_{66}, \quad W_a = d W(0), \quad n_a = d n_v , \tag{B15}$$

yielding

$$F_p d = B J_c d = W_a / a_0 \mu , \tag{B16}$$

$$R_c = a_0 \mu / W_a^{1/2} . \tag{B17}$$

Equation (B16) predicts the pinning force per unit area to be independent of thickness, as expected for 2D pinning. For (B17) we can write

$$\frac{R_c}{a_0} = \left[\frac{\langle u \rangle}{a_0} \right]^{-1} , \tag{B18}$$

in which

$$\langle u \rangle \equiv \langle f_\Phi \rangle / \mu \tag{B19}$$

and

$$\langle f_\Phi \rangle \equiv (n_a a_0^2)^{1/2} \langle f^2 \rangle^{1/2} \tag{B20}$$

are to be interpreted as the net displacement $\langle u \rangle$ of an individual flux line due to the net force $\langle f_\Phi \rangle$ exerted by the pinning centers it encounters. Hence, the relative correlation length is inversely proportional to the relative net displacement of individual flux lines.

*Permanent address: Kamerlingh Onnes Laboratory, University of Leiden, P.O. Box 9506, 2300-RA Leiden, The Netherlands.

[1] P. H. Kes and C. C. Tsuei, Phys. Rev. Lett. 47, 1930 (1981).

[2] A. I. Larkin and Yu. Ovchinnikov, J. Low Temp. Phys. 34, 409 (1979).

[3] A. I. Larkin, Zh. Eksp. Teor. Fiz. 58, 1466 (1970) [Sov. Phys.—JETP 31, 784 (1970)].

[4] Y. Imry and S.-k. Ma, Phys. Rev. Lett. 35, 1399 (1975); P.

Lacour-Gayet, and G. Toulouse, J. Phys. (Paris) 35, 425 (1974).
[5]K. Binder, Y. Imry, and E. Pytte, Phys. Rev. B 24, 6736 (1981).
[6]R. Labusch, Cryst. Lattice Defects 1, 1 (1969).
[7]A. M. Campbell and J. E. Evetts, Adv. Phys. 21, 199 (1972).
[8]E. J. Kramer, J. Nucl. Mater. 72, 5 (1978); J. Appl. Phys. 49, 742 (1978).
[9]H. R. Kerchner, J. Narayan, D. K. Christen, and S. T. Sekula, Phys. Rev. Lett. 44, 1146 (1980).
[10]G. P. van der Meij, Ph.D. thesis, University of Leiden (1984) (unpublished); G. P. van der Meij and P. H. Kes (unpublished).
[11]E. H. Brandt, J. Low Temp. Phys. 26, 709 (1977); 26, 735 (1977); 28, 263 (1977); 28, 291 (1977).
[12]J. M. Kosterlitz and D. J. Thouless, J. Phys. C 6, 1181 (1973); J. M. Kosterlitz, *ibid.* 7, 1046 (1974).
[13]B. I. Halperin and D. R. Nelson, Phys. Rev. Lett. 41, 121 (1978); D. R. Nelson and B. I. Halperin, Phys. Rev. B 19, 2457 (1979).
[14]D. S. Fisher, Phys. Rev. B 22, 1190 (1980).
[15]P. Chaudhari, J. Phys. (Paris) C 8, 267 (1980); P. Chaudhari, F. Spaepen, and P. J. Steinhardt, in Glassy Metals II, edited by H. J. Guntherodt and H. Beck (Springer, Berlin, in press).
[16]H. Kronmüller, J. Appl. Phys. 52, 1859 (1981).
[17]G. S. Cargill and C. C. Tsuei, in *Rapidly Quenched Metals III,* edited by B. Cantor (The Metals Society, London, 1978), p. 337.
[18]C. C. Tsuei, in *Superconducting Materials Science,* edited by S. Foner and B. Schwartz (Plenum, New York, 1981), p. 735.
[19]C. C. Tsuei, S. von Molnar, and J. M. Coey, Phys. Rev. Lett. 41, 664 (1978).
[20]N. Toyota, T. Fukase, A. Inoue, Y. Takahashi, and T. Masumoto, in Proceedings of the 16th International Conference on Low Temperature Physics, edited by P. deChatel and M. Durieux [Physica 107B, 465 (1981)].
[21]E. H. Brandt, J. Low Temp. Phys. 42, 557 (1981).
[22]B. M. Clemens and W. L. Johnson J. Appl. Phys. 53, 7612 (1982).
[23]T. W. Barbee and D. C. Keith, in Stanford SSRL Report No. 7804, edited by H. Winick and G. Brown (unpublished), Vol. III, p. 26.
[24]M. Pomerantz and A. Segmüller, Thin Solid Films 68, 33 (1980); E. Spiller and A. Segmüller, Appl. Phys. Lett. 37, 1048 (1980).
[25]N. R. Werthamer, E. Helfland, and P. C. Hohenberg, Phys. Rev. 147, 295 (1966).
[26]E. H. Brandt, Phys. Status Solidi B 77, 551 (1976).
[27]D. Weaire, M. F. Ashby, J. Logan, and M. J. Weins, Acta Metall. 19, 779 (1971).
[28]H. S. Chen, J. Appl. Phys. 49, 3289 (1978).
[29]J. R. Clem, in *Inhomogeneous Superconductors—1979, (Berkeley Springs, WV),* Proceedings of the Conference on Inhomogeneous Superconductors, edited by T. L. Francavilla, D. V. Gubser, J. R. Leibowitz, and S. A. Wolf (AIP, New York, 1979), p. 245; Phys. Rev. B 9, 898 (1974); 12, 1742 (1975); J. Low Temp. Phys. 18, 427 (1975).
[30]J. Pearl, in *Proceedings of the 9th Conference on Low Temperature Physics, Columbus, Ohio, 1964,* edited by J. G. Daunt, D. O. Edwards, F. J. Milford, and M. Yagub (Plenum, New York, 1965), p. 506.
[31]M. R. Beasley, J. E. Mooij, and T. P. Orlando, Phys. Rev. Lett. 42, 1165 (1979).
[32]A. H. Cottrell, in *Dislocations and Plastic Flow in Crystals* (Clarendon, Oxford, 1953).
[33]D. S. Fisher, B. I. Halperin, and R. Morf, Phys. Rev. B 20, 4692 (1979).
[34]A. T. Fiory, Phys. Rev. B 7, 1881 (1973); 7, 5040 (1973).
[35]B. M. Clemens, W. L. Johnson, J. Bennett, J. Appl. Phys. 51, 1116 (1980); A. Inoue, S. Sakai, H. Kimura, T. Masumoto, and A. Hoshi, Scripta Metall. 14, 235 (1980).
[36]C. C. Koch, J. O. Scarbrough, D. M. Kroeger, and A. DasGupta, Appl. Phys. Lett. 37, 451 (1980); C. C. Koch, J. O. Scarbrough, and D. M. Kroeger, *Proceedings of the 4th International Conference on Rapidly Quenched Metals, Sendai, Japan, 1981,* edited by T. Masumoto and K. Suzuki (The Metals Society, Sendai, Japan, 1982), p. 1229.
[37]D. Srolovitz, K. Maeda, V. Vitek, and T. Egami, Philos. Mag. A 44, 847 (1981); D. Srolovitz, T. Egami, and V. Vitek, Phys. Rev. B 24, 6936 (1981).
[38]P. Chaudhari, A. Levi, and P. Steinhardt, Phys. Rev. Lett. 43, 1517 (1979).
[39]H. Kronmüller, M. Fähnle, M. Domann, H. Grimm, R. Grimm, and B. Gröger, J. Magn. Magn. Mat. 13, 53 (1979).
[40]C. S. Pande, Appl. Phys. Lett. 28, 462 (1976).
[41]E. J. Kramer, Philos. Mag. 33, 331 (1976).
[42]R. Labusch, Phys. Rev. 170, 470 (1968).
[43]H. R. Kerchner, Physica 107B, 463 (1981).
[44]E. J. Kramer, H. C. Freyhardt, J. Appl. Phys. 51, 4903 (1980).
[45]E. V. Thuneberg, J. Kurkijärvi, and D. Rainer, Phys. Rev. Lett. 48, 1853 (1982).
[46]H. Rohrer, Helv. Phys. Acta 33, 675 (1960).
[47]G. A. Alers and D. L. Waldorf, Phys. Rev. Lett. 6, 677 (1961).
[48]T. Egami, N. Y. Acad. Sci. 371, 238 (1981).
[49]A. J. Drehman and W. L. Johnson, Phys. Status Solidi A 52, 499 (1979).
[50]R. E. Elmquist and S. J. Poon, Solid State Commun. 41, 221 (1982).
[51]W. L. McMillan, Phys. Rev. B 167, 331 (1968).
[52]L. P. Gor'kov, Zh. Eksp. Teor. Fiz. 36, 1918 (1959) [Sov. Phys.—JETP 9, 1364 (1959); 37, 1407 (1959) [10, 998 (1960)].
[53]G. Eilenberger and V. Ambegoakar, Phys. Rev. 158, 332 (1967).
[54]See, e.g., M. Tinkham, in *Introduction to Superconductivity* (McGraw-Hill, New York, 1975).
[55]Y. Imry (private communication).
[56]I. S. Gradshteyn and I. M. Ryznick, *Tables of Integrals, Series and Products* (Academic, New York, 1965).
[57]E. A. Chistowa, Izdat, Akad. Nauk SSSR, Moskow, 1958; Translation: Tables of Bessel Functions and Integrals derived from them (Pergamon, New York, 1959).